$$q_m = q_r\delta_{m0} - h_0\left(\frac{1}{2}\frac{k_1}{k_0} - \frac{h_1}{h_0}\right)\phi_{m-1}' - h_0\left(\frac{1}{3}\frac{k_2}{k_0} - \frac{h_2}{h_0}\right)\phi_{m-2}'' - h_0\theta_a - h_1\theta_a\theta_{m-1} - h_2\theta_a\theta_{m-2} \quad (9)$$

$$\theta_m = -\tfrac{1}{2}(k_1/k_0)\phi_{m-1}' - \tfrac{1}{3}(k_2/k_0)\phi_{m-2}'' + \psi_m \quad (10)$$

$$\phi_m' = \sum_{n=0}^{m} \theta_{m-n}\theta_n \quad (11)$$

$$\phi_m'' = \sum_{n=0}^{m} \phi_{m-n}'\theta_n \quad (12)$$

$$\theta = \sum_{m=0}^{\infty} \epsilon^m\theta_m \quad (13)$$

This theorem is proved through introducing Eqs. (4) and (13) into Eqs. (1–3) and singling out coefficients of ϵ, which give a set of linear equations, containing products of derivatives to the functions θ_m. These products are removed by introducing Eq. (10), which considerably simplifies the problem and leads to Eqs. (5–9), containing only time derivatives of the products of θ_m.

In order to predict the convergence of the series (13), consider the general heat flow problem:

$$k_0T_{,ii} + Q = \rho c_0(\partial T/\partial t) \text{ in V} \quad (14)$$

$$k_0T_{,i}\nu_i + h_0T + q = 0 \text{ on B} \quad (15)$$

$$T = 0 \text{ at } t = 0 \quad (16)$$

If $Q \geq 0$ and $q \leq 0$ then from energy considerations $T \geq 0$ and the following theorem can be stated:

Theorem 2

Let T' be a solution to the heat flow problem Eqs. (14–16) with Q' an arbitrary constant and $q' = 0$, let T'' be the corresponding solution with $Q'' = 0$ and q'' an arbitrary constant. If in Eqs. (14–16)

$$q_m \leq q \leq q_M \quad (17)$$

$$Q_m + \rho c_0\frac{T'}{Q'}\frac{\partial Q_m}{\partial t} + \rho c_0\frac{T''}{q''}\frac{\partial q_M}{\partial t} \leq Q \leq Q_M + \rho c_0\frac{T'}{Q'}\frac{\partial Q_M}{\partial t} + \rho c_0\frac{T''}{q''}\frac{\partial q_m}{\partial t} \quad (18)$$

then at all times $t \geq 0$

$$(Q_m/Q')T' + (q_M/q'')T'' \leq T \leq (Q_M/Q')T' + (q_m/q'')T'' \quad (19)$$

The theorem is proved through the introduction of the fictitious temperatures

$$T_M = (Q_M/Q')T' + (q_m/q'')T'' - T \quad (20)$$

$$T_m = (Q_m/Q')T' + (q_M/q'')T'' - T \quad (21)$$

into Eqs. (14–16). Using Eqs. (17) and (18) it follows that $T_M \geq 0$ and $T_m \leq 0$, which proves Eq. (19).

The theorem proved previously, giving bounds on the solution to the linear heat flow problem, can be used to predict the magnitude of the function ψ_{m+1} once ψ_m has been solved from Eqs. (5–7) and the corresponding heat flows Q_{m+1} and q_{m+1} from Eqs. (8) and (9).

Example

The theory outlined previously is applied to the problem of finding the transient temperature field in a convectively heated plate of inconel, having the following material properties, ($\theta = T - 273°\text{K}$): $\rho = 8250$ kg/m^3, $k = 14.7 + 0.015\ \theta$W/m°K, and $c = 430 + 0.265\ \theta$Ws/kg°K. The ambient temperature θ_a and the heat-transfer coefficient h are taken as $\theta_a = 700°\text{K}$ and $h = 190 + 0.029\ \theta$W/m^2°C. The thickness of the plate is taken to be $\delta = 3$ mm with no heat production within it and no heat flux at the surface, i.e., $Q = q_r = 0$.

The solution θ_0 for temperature-independent material properties is derived first and introduced into Eqs. (8) and (9) to give the intermediate heat flows Q_1 and q_1. After having chosen bounds on these functions so that the relations (17) and (18) are satisfied, the corresponding bounds on the function ψ_1 are obtained from Eq. (19) once ψ_1' and ψ_1'' have been solved from Eqs. (14–16). Lastly the function ψ_1 itself is derived from Eqs. (5–7) and a second approximation, $m = 1$, of the temperature field obtained from Eqs. (10–13).

The calculations have been carried out for a chosen value of $\epsilon = 0.01$ and with the following bounds on the heat flows: $Q_m = 0$, $Q_M = Q_1$, $q_m = q_1$, and $q_M = -10^6(1 - e^{-0.035t})$. The found time histories of the function ψ_1 and the temperature field in the middle of the plate are shown in Figs. (1) and (2) below, the solutions of the linear differential equations being taken from Ref. 5.

References

[1] Trostel, R., "Stationäre Wärmespannungen mit temperaturabhängigem Stoffwerten," Ingenieur-Archiv, 1958, p. 416.

[2] Ismail, I. A. and Nowinski, J. L., "Thermoelastic Problems for Shells of Revolution Exhibiting Temperature-Dependent Properties," *Applied Sciences Research*, Vol. 14, No. 3, 1964/1965, p. 211.

[3] Boley, B. A. and Weiner, J. K., *Theory of Thermal Stresses*, Wiley, New York, 1960, Ch. 6, p. 188.

[4] Appl, F. C. and Hung, H. M., "A Principle for Convergent Upper and Lower Bounds," *International Journal of Mechanical Sciences*, Vol. 6, 1964, p. 381.

[5] Carslaw, H. C. and Jaeger, J. C., "Conduction of Heat in Solids," 2nd ed., Oxford University Press, Oxford, Cambridge, Mass., 1959, Chap. 3.

A Simple Linear Approximation for Perturbed Motion about Moderately Elliptic Orbits

ALAN M. SCHNEIDER* AND HOWARD M. KOBLE†

University of California at San Diego, La Jolla, Calif.

IN this Note, the linearized perturbation equations for a circular reference trajectory are applied to elliptic reference trajectories of small eccentricity. The concept is appealing because the closed form solution for the circular reference is so much simpler than the solution for the elliptic case. A numerical example indicates that the accuracy of the circular reference solution is more than adequate for many practical applications. An analysis is outlined to extend the results of the numerical example.

The linear, constant-coefficient differential equations that describe the perturbed motion of a body P relative to a reference body O in a circular orbit are well known.[1–3] The solution to these equations, which for brevity will be called the circular solution, is usually written in terms of coordinates in a local vertical coordinate system centered at O. The circular solution, which contains sines and cosines and terms linear in time, is simple enough to be calculated by hand. It has di-

Received October 15, 1969; revision received June 24, 1970. This research was supported by NASA under Grant NGR-05-009-106.

* Professor of Aerospace Engineering, Department of the Aerospace and Mechanical Engineering Sciences. Associate Fellow AIAA.

† National Science Foundation Trainee, Department of the Aerospace and Mechanical Engineering Sciences.

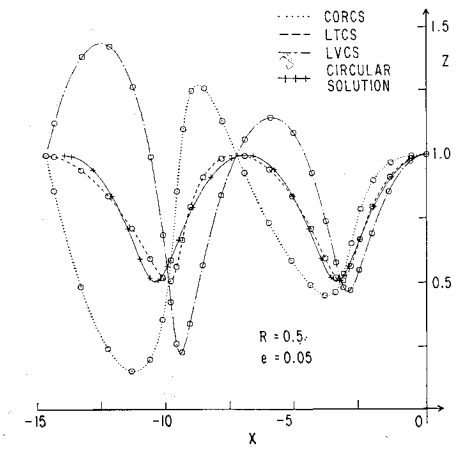

Fig. 1 Comparison of in-plane trajectory of perturbed body in three candidate coordinate systems with circular solution.

rect geometrical interpretation in terms of a point on an interior or exterior radius of a rolling disc. This simplicity makes the equations attractive for use in many applications. In Ref. 3, for example, they form the basis for constructing a manual guidance scheme for rendezvous, in which the nonmaneuvering target is the reference body and the interceptor is the perturbed body. This Note extends their use by showing that an interpretation of the coordinates exists for elliptic reference orbits such that the circular solution adequately defines the observed perturbation behavior.‡

Three different coordinate systems were examined for expressing the small perturbations from the elliptic reference orbit. These were designated the local vertical (LVCS), the constant orbital rate (CORCS), and the local tangent (LTCS) coordinate systems. All three are right-handed Cartesian systems centered at O, where the y axis is out of plane, the z axis is more or less in the outward radial direction, and the x axis is more or less in the direction of motion. More precisely, in LVCS, the x axis is normal to the radius vector from the force center to O. In CORCS, x is initially parallel to the x axis of LVCS, but then rotates at a constant rate relative to inertial space, equal to the mean motion of the reference orbit. In LTCS, the x axis is tangent to the reference orbit at O.

The accuracy of the circular solution in describing the motion about an elliptic reference orbit was tested on the digital computer. The simulation used exact equations of motion to propagate the absolute position of both the reference and perturbed body. Test cases were selected spanning the space of all trajectories inherent in the circular solution, in the sense that they cover the full range of the in-plane shape parameter r, defined by $r = z_a/z_b$ where z_a and z_b are the extreme values of z, z_a being the one of smaller absolute value. The change in semimajor axis δa of the perturbed trajectory is linearly related to r by the formula $0.5z_b(r + 1)$. Since the y motion is the same in all three coordinate systems and since it is decoupled from the in-plane motion, only the in-plane or x-z solution is germane.

Samples of the results are shown in Figs. 1–3.§ Figure 1 shows the exact relative in-plane motion of the perturbed body as seen in each of the three coordinate systems. In addition, the circular solution appears for comparison. A value of 0.05 was used as the eccentricity of the reference orbit. One unit is 0.001 nautical mile (nm), and Earth orbits having a 3700 nm semimajor axis are assumed. Tick marks are placed on the trajectories $\frac{1}{12}$ of a reference orbit period apart.

First, it is seen that the circular solution very nearly matches the exact solution in the LTCS. Second, it is noted that the match is better for LTCS than for either LVCS or CORCS. Although not apparent from the data presented here, it was found that the deviation, for given conditions, between the circular solution and the exact trajectory is linear with eccentricity over the range of values tested.

The eccentricity error of the circular orbit equations in a given coordinate system is defined as the value of relative position (x,z) at a given time computed from these equations, minus the exact value of relative position. The eccentricity error Δx and Δz for the three coordinate systems is plotted vs. time t in Figs. 2 and 3, respectively. In order to reduce second order effects, a value of eccentricity equal to 0.01 was chosen for these plots; all other conditions are the same as were used for Fig. 1.

Examination of the complete set of these curves[7] reveals that for any value of r, the x-error at the end of an integral number of orbit periods is nearly the same in all three coordinate systems, but varies linearly from zero to a maximum as r varies from -1 to 1. Hence, the x-error is proportional to δa. In addition, while the z-error of LVCS and CORCS is finite, one being roughly the negative of the other, the z-error of LTCS is essentially zero. The practical elimination of the z-error is, in fact, the key to the improvement of LTCS over the other two coordinate systems.

Straight lines on the x- and z-error plots approximately bound the errors. These lines are drawn from the origin through the points $[t = T, \Delta x \text{ or } \Delta z = \pm e \cdot x(T)]$ where T is the period and e is the eccentricity of the reference orbit. Thus, the error is bounded by a function that grows linearly with time and is proportional to the reference orbit eccentricity. These bounds do not pertain to Δz in LTCS which is essentially zero, as noted previously.

It was pointed out by a reviewer that the proportionality of the error to e and δa, the equality of the x- and z-error bounds and their linearity with time, the apparent cosine and sine behavior in Figs. 2 and 3 respectively, and the essentially zero magnitude of the z-error in LTCS can be summarized in the equations

$$\text{LVCS} \quad \Delta x = -kt(\delta a)e \cos f \tag{1}$$

$$\Delta z = -kt(\delta a)e \sin f \tag{2}$$

$$\text{LTCS} \quad \Delta x = -kt(\delta a)e \cos f \tag{3}$$

$$\Delta z = 0 \tag{4}$$

where f is the true anomaly. Furthermore, he outlined the derivation of these equations and evaluated the constant k from the following theoretical considerations. The primary error in adapting the equations of circular motion to an orbit that is slightly elliptical is caused by the secular terms in the equations. It is appropriate to examine the full state transition

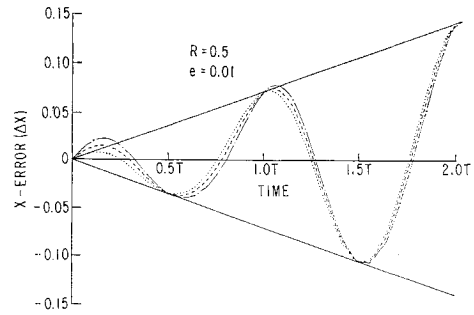

Fig. 2 The eccentricity error of the circular reference orbit solution in the three candidate coordinate systems: x axis.

‡ It should be pointed out that the linearized perturbation equations of motion in an elliptic reference orbit have been solved in closed form.[4–6] However, the elliptic solution is more complicated than the circular solution, and hence the applicability of the latter is investigated.

§ Complete results appear in Ref. 7.

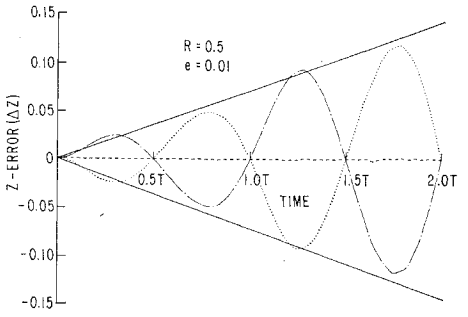

Fig. 3 Eccentricity error of the circular reference orbit solution in the three candidate coordinate systems: z axis.

matrix for an elliptic reference orbit to determine the effect of a small value of eccentricity on these terms. The secular terms are found to be linear in time and also linear in $\delta a/a$. In the local vertical coordinate system (LVCS) of this Note, the secular terms in position variation are

$$x = -1.5V_x t(\delta a)/a \tag{5}$$

$$z = -1.5V_z t(\delta a)/a \tag{6}$$

where

$$V_x = \mu(1 + e\cos f)/h \tag{7}$$

$$V_z = \mu e(\sin f)/h \tag{8}$$

In the local tangent coordinate system (LTCS) the corresponding terms are

$$x = -1.5Vt(\delta a)/a \tag{9}$$

$$z = 0 \tag{10}$$

where

$$V = \mu(1 + 2e\cos f + e^2)^{1/2}/h \tag{11}$$

V_x and V_z are components of reference velocity along the x and z axes, V is the reference velocity magnitude, μ is the gravitation parameter, and h is the angular momentum. To first order in e, the secular errors due to neglecting e are then given by Eqs. (1–4) with $k = 1.5\mu/ha$.

In summary, the circular orbit equations can be used to describe perturbed motion about a moderately elliptic reference orbit if the relative position vector is expressed in a local tangent coordinate system. The accuracy is probably more than adequate for many applications including manual rendezvous in earth orbit, up to an eccentricity of 0.05.

References

[1] Clohessy, W. H. and Wiltshire, R. S., "Terminal Guidance System for Satellite Rendezvous," *Journal of the Aerospace Sciences*, Vol. 27, No. 9, Sept. 1960, pp. 653–658, 674.

[2] Steffan, K. L., "Orbital Guidance," *Guidance of Aerospace Vehicles*, edited by C. T. Leondes, McGraw-Hill, New York, 1963, pp. 426–458.

[3] Schneider, A. M., Prussing, J. E., and Timin, M. E., "A Manual Method for Space Rendezvous Navigation and Guidance," *Journal of Spacecraft and Rockets*, Vol. 6, No. 9, Sept. 1969, pp. 998–1006.

[4] Stern, R. G., "Interplanetary Midcourse Guidance Analysis," Sc.D. thesis, 1963, Dept. of Aeronautics and Astronautics, Massachusetts Institute of Technology.

[5] Alspach, D. L., "Solutions to the Homogeneous Equation for Arbitrary Eccentricity," Subappendix 5 to Appendix XXI of Schneider, A. M., Prussing, J. E., and Timin, M. E., *Manual Techniques for Spacecraft Rendezvous and Reentry*, Rept. AFAL-TR-68-300, Nov. 2, 1968, Air Force Avionics Lab., Wright-Patterson Air Force Base, Ohio.

[6] Tschauner, J., "Elliptic Orbit Rendezvous," *AIAA Journal*, Vol. 5, No. 6, June 1967, pp 1110–1114.

[7] Schneider, A. M. and Koble, H. M., "Eccentricity Error of Dynamical Equations Linearized about a Circular Orbit," Rept. SDC-1-69, Aug. 18, 1969, Dept. of Aerospace and Mechanical Engineering Sciences, University of California at San Diego; also Revision A, May 1, 1970.

Random Vibration Response of Cantilever Plates Using the Finite Element Method

ALFRED T. JONES* AND CHARLES W. BEADLE†
University of California, Davis, Calif.

Nomenclature

E	= Young's modulus, lbf/in.^{2}
f_n	= nth generalized force, lbf
$f(x,y,t)$	= driving force, lbf
$H(\omega)$	= frequency transfer function, g/lbf
m_n	= nth generalized mass, lbf-sec^2/in.
N	= total number of data points used in spectral analysis
PSD	= power spectral density
$S_a(\omega)$	= acceleration spectral density, g^2/cps
$S_f(\omega)$	= driving force spectral density, lbf^2/cps
T	= total time length of signal segment used in spectral analysis, sec
t	= time, sec
$\{w\}$	= $n \times 1$ column matrix representing discretized plate displacement
ζ_n	= nth modal damping ratio
ω_n	= nth natural frequency
ν	= Poisson's ratio
$\{\Phi_n\}$	= $n \times 1$ column matrix representing nth eigenvector
Ψ_n	= nth phase angle
τ	= sampling period, sec

Introduction

ANALYSIS of structures subjected to random excitation has become an important problem. With deterministic excitation, an undamped model was usually sufficient to describe motion, but random signals have energy present in most

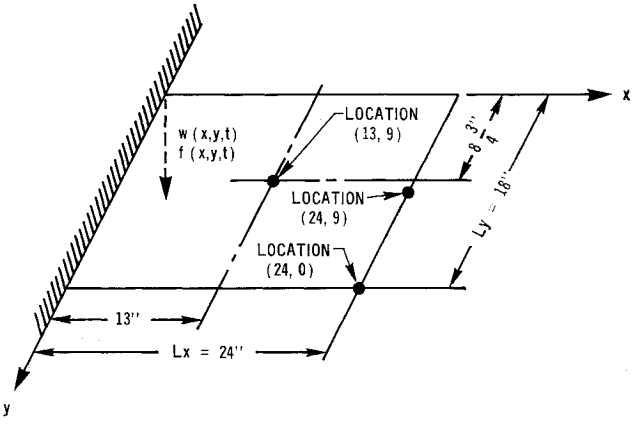

Fig. 1 Plate and coordinate system.

Received December 11, 1969; revision received May 27, 1970.

* Presently Staff member, Sandia Laboratories, Livermore, Calif.

† Associate Professor of Mechanical Engineering.